NANOSTRUCTURED MATERIALS AS CATALYSTS FOR THE PRODUCTION OF GASOLINE FROM USED PALM OIL AND CRUDE PALM OIL: SYNTHESIS, CHARACTERIZATION AND ACTIVITY STUDIES

NOOR AISYAH AHMAD SHAH

UNIVERSITI SAINS MALAYSIA

2007

NANOSTRUCTURED MATERIALS AS CATALYSTS FOR THE PRODUCTION OF GASOLINE FROM USED PALM OIL AND CRUDE PALM OIL: SYNTHESIS, CHARACTERIZATION AND ACTIVITY STUDIES

by

NOOR AISYAH AHMAD SHAH

Thesis submitted in fulfillment of the requirements for the degree of Master of Science

MARCH 2007

ACKNOWLEDGEMENTS

Thanks to Allah the Al-Mighty for His blessing during my Master study and grants me the ability to complete this study. Afterwards, I would like to express my special appreciation to my supervisor, Professor Subhash Bhatia for his excellent and patient guidance and infinite suggestions and help throughout this research work. Special thanks also to my co-supervisor, Professor Abdul Rahman Mohamed for his help and advice during my postgraduate study in School of Chemical Engineering, USM.

I would also like to show my gratitude to the Dean of School of Chemical Engineering for the support and research facilities available in the school. The financial support by Long Term IRPA Grant from MOSTI and USM Graduate Assistant allowance is gratefully appreciated. I would also like to wish thank you to all administrative staff and technicians in the school for their valuable help. Not forgotten, technicians in School of Chemical Sciences for FTIR and Nitrogen Adsorption analysis, School of Physics for XRD analysis, and School of Biological for SEM analysis. Thanks for being so helpful.

Last but not least, my deepest gratitude to my beloved parents, sisters and brother for their endless love, blessing and support. Thanks a lot for always standing by me. To all my friends, Cheng Teng, Zalina, Chua, Tan, Yean Sang, Pramila, Hairul, Hanida, Aziah, Fakar, Zali, Zahrah, Huda, Dila and others, thank you very much for your sincere help, concern, moral support and kindness.

TABLE OF CONTENTS

		Page
ACKNOWLEDGEMENTS		ii
TABLE OF CONTENTS		iii
LIST OF TABLES		vii
LIST OF FIGURES		ix
LIST OF SYMBOLS		xii
LIST OF ABBREVIATION		xiii
ABSTRAK		xv
ABSTRACT		xviii
CHAPTER 1: INTRODUCTION		
1.1	Petroleum Resources	1
1.2	Alternative Fuels for Future	1
1.3	Biofuel from Palm Oil	2
1.4	Nanostructured Cracking Catalysts	4
1.5	Problem Statement	6
1.6	Objectives	7
1.7	Scope of the Study	7
1.8	Organization of the Thesis	9
CHAPTER 2: LITERATURE REVIEW		
2.1	Zeolite, Molecular Sieves and Nanostructured Materials	11
	2.1.1 Microporous Materials	13
	2.1.1 (a) Zeolite	14
	ZSM-5	15
	Zeolite Beta	16
	2.1.1 (b) Zeolite as Cracking Catalyst	17
	ZSM-5	18
	Zeolite Beta	19
	2.1.2 Mesoporous Materials	19
	2.1.2 (a) MCM-41	20
	2.1.2 (b) SBA-15	21
	2.1.2 (c) Physicochemical Properties of Mesoporous Materials	21
	Crystallinity	21
	Acidity	22

Hydrothermal stability 23
2.1.2 (d) Performances of Mesoporous Materials 25
MCM-41 25
SBA-15 26
2.1.3 Composite Materials 26
2.1.3 (a) Bimodal Pore System of Active Material with Less Active Material 26
2.1.3 (b) Bimodal Pore System of Active Materials 28
2.2 Characterization of Catalyst 33
2.2.1 Physical Properties 33
2.2.1 (a) Surface Area, Pore Size Distribution and Adsorption-desorption Isotherm 33
2.2.1 (b) X-ray Diffraction (XRD) Crystallography 34
2.2.1 (c) Microscopy 35
2.2.2 Chemical Properties 35
2.2.2 (a) Determination of Acidity 35
2.3 Catalytic Cracking of Vegetable Oils 36
2.4 Deactivation Studies 42

CHAPTER 3: EXPERIMENTAL METHODS AND ANALYSIS

3.1 Materials and Chemicals 45
3.1.1 Palm Oil 45
3.1.2 Zeolite 46
3.1.2 (a) HZSM-5 46
3.1.2 (b) H-Beta 47
3.1.3 Chemicals and Reagents 47
3.2 Experimental Methods and Analysis 48
3.2.1 Catalyst Preparation 49
3.2.1 (a) Mesoporous Materials 49
MCM-41 49
SBA-15 49
Post-Synthesis Alumination of SBA-15 50
3.2.1 (b) Composite Materials 51
Composite microporous/mesoporous materials-Alumina 51

Composite microporous/mesoporous materials-Silica-alumina 54

3.2.2 Catalyst Characterization 55

3.2.2 (a) Nitrogen Adsorption 55

3.2.2 (b) X-Ray Diffraction (XRD) 56

3.2.2 (c) Scanning Electron Microscopy (SEM) 56

3.2.2 (d) Fourier Transform Infrared (FTIR) Spectroscopy 57

3.2.2 (e) Thermal Gravimetric Analysis (TGA) 57

3.2.3 Hydrothermal Stability Test 57

3.2.4 Catalyst Activity Measurement 58

3.2.4 (a) Activity Test 58

3.2.4 (b) Deactivation (Time on Stream) Studies 60

3.2.4 (c) Reusability Studies 60

3.2.5 Product Analysis 61

3.2.5 (a) Liquid Products 61

3.2.5 (b) Gaseous Product 61

CHAPTER 4: RESULTS AND DISCUSSION

4.1 Catalyst Characterization 63

4.1.1 Zeolite HZSM-5 64

4.1.1 (a) Composite HZSM-5/Alumina (CZA) 64

4.1.2 Zeolite H-Beta 76

4.1.2 (a) Composite H-Beta/Silica-alumina (CBS) 76

4.1.2 Mesoporous Materials 83

4.1.2 (a) Al-SBA-15 prepared by Post-Synthesis Alumination 83

4.1.2 (b) Al-SBA-15 vs Al-MCM-41 (Prepared by Direct Synthesis Alumination) 86

4.1.2 (c) Composite Al-MCM-41 with alumina (CMA) and silica-alumina (CMS) 88

4.1.2 (d) Composite Al-SBA-15 with alumina (CSA) and silica-alumina (CSS) 92

4.2 Catalytic Activity 96

4.2.1 Composite HZSM-5/Alumina (CZA) 98

4.2.1 (a) HZSM-5 vs Composite HZSM-5/Alumina (CZA) vs Alumina 98
4.2.1 (b) Hydrothermal stability study 102
4.2.1 (c) Reusability study 104
4.2.1 (d) Physical mixture (PZA35) vs composite CZA35 106
4.2.1 (e) Deactivation (Time on stream) study 107
4.2.2 Composite H-Beta/Silica-alumina (CBS) 110
4.2.2 (a) H-Beta vs Composite H-Beta/Silica-alumina (CBS) vs Silica-Alumina 110
4.2.2 (b) Hydrothermal stability study 112
4.2.2 (c) Physical mixture (PBS25) vs Composite CBS25 113
4.2.2 (d) Deactivation (Time on stream) study 114
4.2.3 Al-SBA-15 Prepared by Post-Synthesis Alumination method 115
4.2.4 Mesoporous materials and their composite with alumina and silica-alumina 117
4.2.4 (a) Al-MCM-41 vs Al-SBA-15 118
4.2.4 (b) Al-MCM-41 vs steam treated Al-MCM-41 (St-AlMCM-41) 119
4.2.4 (c) Al-SBA-15 vs steamed Al-SBA-15 (St-AlSBA-15) 120
4.2.4 (d) St-AlMCM-41 vs St-AlSBA-15 120
4.2.4 (e) Composite Al-MCM-41/Alumina (CMA) 120
4.2.4 (f) Composite Al-SBA-15/Alumina (CSA) 122
4.2.4 (g) Composite Al-MCM-41/silica-alumina (CMS) 123
4.2.4 (h) Composite Al-SBA-15/silica-alumina (CSS) 123
4.2.4 (i) Deactivation (Time on stream) study over Al-MCM-41 and CMA25 124
4.3 Deactivation Studies 126

CHAPTER 5 : CONCLUSIONS AND RECOMMENDATIONS 134
5.1 Conclusions 134
5.2 Recommendations 136

REFERENCES 137

APPENDICES
Appendix A Organic liquid product analysis 146
Appendix B Gaseous Products Analysis 147

LIST OF TABLES

		Page
Table 2.1	Important groups of inorganic microporous materials (Vaughan, 1989).	14
Table 2.2	Composite catalysts of porous materials.	31
Table 3.1	Fatty acid composition of UPO and CPO (RBD palm oil).	46
Table 3.2	List of chemicals and reagents.	47
Table 3.3	List of different analytical techniques used to characterize the different catalysts properties.	55
Table 4.1	Physicochemical properties of HZSM-5, its composite CZA and their steam treated samples.	66
Table 4.2	Physicochemical properties of H-Beta, its composite CBS25 and their steam treated samples (St-Beta and St-CBS25).	78
Table 4.3	Lattice *d* spacing and cell parameter of SBA-15 and various Al-SBA-15.	84
Table 4.4	Catalytic cracking of used palm oil (UPO) and crude palm oil (CPO) over HZSM-5.	97
Table 4.5	Catalytic cracking of used palm oil (UPO) over HZSM-5, CZA10, CZA20, CZA35, CZA60, CZA85, PZA35, alumina, steamed HZSM-5 and steamed composite CZA35 catalysts.	99
Table 4.6	Catalytic cracking of used palm oil over HZSM5 and its regenerated catalyst for five times.	104
Table 4.7	Catalytic cracking of used palm oil over CZA35 and its regenerated catalyst for six times.	105
Table 4.8	Catalytic cracking of crude palm oil (CPO) over HBeta, CBS5, CBS15, CBS25, PBS25, silica-alumina, steamed H-Beta and steamed composite CBS25 catalysts.	110
Table 4.9	Catalytic cracking of crude palm oil (CPO) over SBA-15, AlSBA(20), AlSBA(P1), AlSBA(P2) and AlSBA(P3).	115
Table 4.10	Catalytic cracking of crude palm oil over Al-MCM-41, their composite with alumina, CMA25 and CMA35; with silica-alumina, CMS25 and steam treated samples.	118
Table 4.11	Catalytic cracking of crude palm oil over Al-SBA-15, their composite with alumina, CSA25 and CSA35; with silica-alumina, CSS25 and steamed treated samples.	118

Table 4.12 Different types of activity models proposed for different values of catalyst deactivation order, n_d.. 128

Table 4.13 The values of correlation coefficient, R^2, activity order, n_d, activity rate constant, k_d and sum of squares, $\sum s^2$. 128

Table 4.14 Deactivation rate constant, k_d, deactivation order, n_d, experimental activity, φ (Exp.), activity determined using chosen model, φ (Model) and the sum of squares, $\sum s^2$ for palm oil cracking over different catalysts at reaction temperature of 723 K and WHSV of 2.5 h^{-1}. 130

LIST OF FIGURES

		Page
Figure 1.1	World major producers of palm oil 2004 (MPOB, 2006b).	3
Figure 2.1	Framework structure of ZSM-5 (Gates, 1992).	16
Figure 2.2	Pore structure in BEA along *b* (left) and *a* (right) axis (Iza-Structure, 2006).	17
Figure 2.3	Hexagonal structure of mesoporous materials.	20
Figure 2.4	Schematic diagram of the composite pellet.	27
Figure 2.5	Schematic diagram of the core-shell composite.	28
Figure 2.6	Proposed reaction pathway for the conversion of vegetable oils over zeolite cracking catalysts (Katikaneni *et al.*, 1995; Leng *et al.*, 1999).	38
Figure 3.1	Flowchart of overall experimental plan.	48
Figure 3.2	Model of a granular composite microporous (HZSM-5) or mesoporous materials/alumina	52
Figure 3.3	Flowchart for the preparation of composite microporous or mesoporous materials/alumina and the granulation process.	52
Figure 3.4	Model of a particle of composite Silica-alumina/zeolite (H-Beta) or mesoporous materials.	55
Figure 3.5	Schematic diagram of micro-reactor rig used in catalytic cracking of fatty acids mixture and UPO.	59
Figure 4.1	Different types of catalysts used in the cracking of CPO and UPO.	63
Figure 4.2	XRD images of HZSM-5 and composite HZSM-5/Alumina (CZA) with different percentage of alumina coating.	65
Figure 4.3	Isotherms of nitrogen sorption for HZSM-5 and composite HZSM-5/Alumina (CZA) with different alumina weight percentages of fresh catalysts.	68
Figure 4.4	Isotherms of nitrogen sorption for (a) steam treated catalyst (St-ZSM5 and St-CZA35) and spent CZA35 catalyst after being regenerated and reused (CZA35-RegVI) for six times, (b) comparison St-ZSM5 with fresh HZSM5 and (c) comparison St-CZA35 with fresh CZA35.	69
Figure 4.5	Pore size distributions of HZSM-5 and composite HZSM-5/Alumina (CZA) with different weight percentage of alumina coating of fresh catalysts.	70

Figure 4.6	Pore size distributions of (a) steam treated catalyst (St-ZSM5 and St-CZA35) and spent CZA35 catalyst after being regenerated and reused (CZA35-RegVI) for six times, (b) comparison St-ZSM5 with fresh HZSM5 and (c) comparison St-CZA35 with fresh CZA35.	71
Figure 4.7	FTIR spectra of pyridine adsorbed HZSM-5 and its composite CZA catalysts withHZSM-5/Alumina different percentage of alumina coating, with L: Lewis site and B: Brønsted site.	72
Figure 4.8	SEM images of (a) uncoated HZSM-5, and (b) after being coated with 35 wt% alumina, CZA35.	73
Figure 4.9	SEM image of (a) full granular fresh composite CZA35, (b) full granular regenerated CZA35 for 6 times (CZA35-RegVI).	74
Figure 4.10	Thermal gravimetric analysis of fresh HZSM-5 and CZA35.	75
Figure 4.11	XRD diffractograms of H-Beta and composite H-Beta/Silica-alumina at 25 wt% silica-alumina amount (CBS25).	77
Figure 4.12	Nitrogen adsorption-desorption isotherms, and (b) pore size distributions of uncoated H-Beta, composite H-Beta/silica-alumina (CBS25) and their steam treated samples (St-Beta and St-CBS25).	79
Figure 4.13	SEM micrograph of (a) uncoated H-Beta at magnification of 10 K X (b) CBS15 at magnification of 5 K X and (c) CBS25 at magnification of 5 K X.	81
Figure 4.14	FTIR for the pyridine-adsorbed samples.	82
Figure 4.15	Powder X-ray diffraction patterns of purely siliceous SBA-15 and different types of Al-SBA-15 samples.	84
Figure 4.16	FTIR spectra of pyridine adsorbed on purely siliceous SBA-15 and various Al-SBA-15.	85
Figure 4.17	XRD patterns of Al-SBA-15 and Al-MCM-41 in the low angle 2θ region.	86
Figure 4.18	SEM image of (a) Al-SBA-15 at magnification of 5 K and (b) Al-MCM-41 at magnification of 15 K.	87
Figure 4.19	FTIR for the pyridine-adsorbed Al-MCM-41 and Al-SBA-15.	88
Figure 4.20	XRD patterns of Al-MCM-41, composite CMA25 and CMS25 in the 2θ low angle region.	89
Figure 4.21	SEM images of composite Al-MCM-41 with (a) alumina (CMA25) at magnification of 2 K and (b) silica-alumina (CMS25) at magnification of 15 K.	90
Figure 4.22	FTIR for the pyridine-adsorbed Al-MCM-41, its composites: CMA25 and CMS25; alumina and silica-alumina.	91

Figure 4.23	Thermal gravimetric analysis (TGA) for Al-MCM-41 and its composite with alumina, CMA25.	92
Figure 4.24	XRD patterns of Al-SBA-15, composite CSA25 and CSS25 in the low angle 2θ region.	93
Figure 4.25	SEM images of composite Al-SBA-15 with (a) alumina (CSA25) at magnification of 2 K and (b) silica-alumina (CSS25) at magnification of 10 K.	94
Figure 4.26	FTIR spectra of the pyridine adsorbed Al-SBA-15 and their composites: CSA25 and CSS25, and silica-alumina.	95
Figure 4.27	Effect of alumina content in the composite catalysts over the yields of gasoline, OLP, coke and gas.	102
Figure 4.28	Selectivity of fresh and steam treated HZSM-5 and composite CZA35 towards different OLP fractions, gaseous, water, coke yields and aromatics content in OLP fraction.	103
Figure 4.29	Products distribution of composite CZA35 (──) and HZSM-5 (----) after being regenerated and reused in the palm oil cracking.	106
Figure 4.30	Effect of the time on stream and regeneration for the conversion of used palm oil cracking over HZSM-5, composite HZSM-5/Alumina, CZA35 and their physical mixture, PZA35.	108
Figure 4.31	Effect of the time on stream and regeneration for the gasoline fraction yield of used palm oil cracking over HZSM-5, composite HZSM-5/Alumina, CZA35 and their physical mixture, PZA35.	109
Figure 4.32	Selectivity towards different fraction of OLP over H-Beta, composites CBS and their physical mixture (PBS25) in crude palm oil cracking.	112
Figure 4.33	Effect of the time on stream for the conversion of crude palm oil cracking over H-Beta, composite H-Beta/Silica-lumina, CBS25 and the physical mixture of H-Beta and silica-alumina, PBS25.	114
Figure 4.34	Selectivity of different fraction of OLP over SBA-15 and various Al-SBA-15 in crude palm oil cracking.	117
Figure 4.35	Effect of the time on stream and regeneration for the conversion of crude palm oil cracking over Al-MCM-41 and composite Al-MCM-41/Alumina, CMA25.	124
Figure 4.36	Time on stream for the cracking of palm oil over different types of catalysts.	127
Figure 4.37	Experimental and prediction data of palm oil cracking activity over different catalysts.	132

LIST OF SYMBOLS

φ	Activity
Å	Angstrom Unit
[Al]	Aluminum Concentration
θ	Angle Region (Theta)
B	Brønsted Acid Site
R^2	Coefficient Correlation
n_d	Deactivation Order
k_d	Deactivation Rate Constant
D(v)d	Differential Volume
d_{100}	Lattice *d*(100) Spacing
L	Lewis Acid Site
P/P_0	Relative Pressure
$\sum s^2$	Sum of Squares
Si/Al	Silicon/Aluminum Ratio
t	Time on Stream
a_o	Unit Cell Parameter
λ	Wavelength
wt%	Weight Percentage

LIST OF ABBREVIATION

ALISOP	Aluminum isopropoxide
APS	Average Pore Size
BET	Brunauer-Emmett-Teller
BJH	Barrett-Joyner-Halenda
BTX	Benzene, Toluene and Xylene
CBSX	Composite H-Beta with silica-alumina with X: silica-alumina weight percentage
CMAX	Composite Al-MCM-41 with alumina with X: alumina weight percentage
CMSX	Composite Al-MCM-41 with silica-alumina with X: silica-alumina weight percentage
CPO	Crude Palm Oil
CSAX	Composite Al-SBA-15 with alumina with X: alumina weight percentage
CSSX	Composite Al-SBA-15 with silica-alumina with X: silica-alumina weight percentage
CTABr	Hexadecyltrimethylammonium bromide
CZAX	Composite HZSM-5 with alumina with X: alumina weight percentage
GC-MS	Gas Chromatography-Mass Spectrometry
FID	Flame Ionization Detector
FCC	Fluid Catalytic Cracking
FTIR	Fourier Transform Infrared
MCM	Mobil Crystalline Material
OTC	Oil to Catalyst Ratio
PEO	Poly(ethylene oxide)
PONA	Paraffin, Olefin, Naphta and Aromatic
PSD	Pore Size Distribution
RBD	Refined, Bleached and Deodorized
SEM	Scanning Electron Microscopy

St	Steamed
TCD	Thermal Conductivity Detector
TEOS	Tetra-ethyl orthosilicate,
TGA	Thermal Gravimetric Analysis
TMAOH	Tetra-methyl ammonium hydroxide
TOS	Time on Stream
UPO	Used Palm Oil
WHSV	Weight Hourly Space Velocity
XRD	X-Ray Diffraction
ZSM	Zeolite Socony Mobil

BAHAN BERSTRUKTUR NANO SEBAGAI MANGKIN UNTUK PENGHASILAN GASOLIN DARIPADA MINYAK SAWIT TERPAKAI DAN MINYAK SAWIT MENTAH: KAJIAN SINTESIS, PENCIRIAN DAN AKTIVITI

ABSTRAK

Objektif penyelidikan ini adalah untuk menghasilkan mangkin peretakan yang efisien serta mempunyai kestabilan hidroterma yang baik, kebolehulangan guna semula, kadar penurunan aktiviti yang rendah dan hasil sampingan yang minimum dengan kepilihan tinggi terhadap hasil bahagian gasolin. Oleh itu, proses pemangkinan untuk menghasilkan gasolin daripada minyak sawit mentah dan minyak sawit terpakai telah dikaji pada tekanan atmosfera, suhu 723 K, halaju (WHSV) pada 2.5 jam^{-1} dan nisbah minyak sawit mentah/terpakai terhadap mangkin bersamaan 8 di dalam reaktor mikro lapisan tetap.

Enam jenis mangkin komposit berbeza iaitu; HZSM-5/alumina (CZA), H-Beta/silika-alumina (CBS), Al-MCM-41/alumina (CMA), Al-MCM-41/silika-alumina (CMS), Al-SBA-15/alumina (CSA) dan Al-SBA-15/silika-alumina (CSS) telah disintesis dan diuji sebagai mangkin peretakkan. Komposit CZA dan CBS telah dicirikan untuk luas permukaan, isoterma penjerapan-penyahjerapan, taburan saiz liang, kehabluran, keasidan dan morfologi permukaan. Komposit CMA, CSA, CMS dan CSS telah dicirikan untuk kehabluran, keasidan dan morfologi permukaan.

HZSM-5 memberikan 98.5 % berat penukaran minyak sawit terpakai dengan 45.2 % berat hasil bahagian gasolin dan 25.9 % berat hasil gas. Komposit CZA35 memberikan 97 % berat penukaran minyak sawit terpakai dengan 47 % berat hasil bahagian gasolin dan 19.7% berat hasil gas berbanding dengan HZSM-5. Lapisan alumina telah meningkatkan saiz liang purata liang meso dan menurunkan keasidan mangkin komposit. HZSM-5 dan CZA35 yang dirawat stim menunjukkan aktiviti yang setanding dengan mangkin baru. St-ZSM5 memberikan 93.5 % berat penukaran

minyak sawit terpakai dengan 46.0 % berat hasil bahagian gasolin dan penukaran minyak sawit 92.3 % berat dengan 46.3 % berat hasil bahagian gasolin oleh St-CZA35. Penurunan luas permukaan St-CZA35 adalah lebih rendah berbanding St-ZSM5. Aromatik (BTX) yang terkandung dalam produk cecair organik (OLP) telah dikurangkan daripada 33.9 % berat yang diperolehi oleh CZA35 baru kepada 17.9 % berat oleh St-CZA35.

Komposit CBS25 memberikan hasil bahagian gasolin yang setanding dengan 62.9% berat penukaran minyak sawit mentah berbanding 74.5% berat penukaran minyak sawit mentah oleh H-Beta. Aktivitinya meningkat selepas rawatan stim dengan peningkatan penukaran minyak sawit mentah kepada 74.7% berat dengan 31.8 % berat hasil bahagian gasolin. Aktiviti H-Beta menurun selepas rawatan stim dengan penurunan penukaran minyak sawit mentah daripada 74.5 % berat kepada 65.5 % berat dan hasil bahagian gasolin daripada 26% berat kepada 23.8 % berat. Lapisan silika-alumina telah membantu meningkatkan aktiviti peretakan dan kestabilan hidroterma komposit disebabkan oleh perubahan morfologi permukaan.

Lapisan alumina telah meningkatkan kestabilan hidroterma Al-MCM-41. St-CMA25 telah memberikan 62 % berat penukaran minyak sawit mentah dengan 19.7 % berat hasil bahagian gasolin, iaitu lebih tinggi daripada yang diperolehi oleh St-AlMCM-41 (60.5 % berat penukaran minyak sawit dengan 13.1 % berat hasil bahagian gasolin). Komposit CSA, CMS dan CSS telah memberikan aktiviti peretakan yang rendah disebabkan oleh perubahan morfologi permukaan sebagaimana yang dikesan daripada analisis SEM. Perbandingan prestasi kesemua komposit yang disintesis, CZA35 telah dikenalpasti sebagai mangkin peretakan yang paling baik.

Penurunan aktiviti mangkin telah dikaji dengan memperolehi data masa ketika aliran dengan nisbah minyak sawit terhadap mangkin di dalam julat 8 ke 16. Komposit

dengan alumina, CZA35 and CMA25 menunjukkan penurunan aktiviti yang lebih rendah berbanding mangkin HZSM-5 dan Al-MCM-41. Data penurunan aktiviti ditetapkan menggunakan model yang sesuai dan parameter-parameter penurunan aktiviti telah diperolehi.

NANOSTRUCTURED MATERIALS AS CATALYSTS FOR THE PRODUCTION OF GASOLINE FROM USED PALM OIL AND CRUDE PALM OIL: SYNTHESIS, CHARACTERIZATION AND ACTIVITY STUDIES

ABSTRACT

The objective of this research was to develop an efficient cracking catalyst with good hydrothermal stability, reusability, low deactivation rate and minimum side products with high selectivity towards gasoline fraction yield. In this research, the catalytic process for the production of gasoline from crude palm oil (CPO) and used palm oil (UPO) was studied at atmospheric pressure, temperature of 723 K, weight hourly space velocity (WHSV) of 2.5 h^{-1} and crude/used palm oil to catalyst ratio of 8 in a fixed bed micro-reactor.

Six different types of composite catalysts namely; HZSM-5/alumina (CZA), H-Beta/silica-alumina (CBS), Al-MCM-41/alumina (CMA), Al-MCM-41/silica-alumina (CMS), Al-SBA-15/alumina (CSA) and Al-SBA-15/silica-alumina (CSS) were synthesized and tested as cracking catalysts. The composite CZA and CBS were characterized for their surface area, adsorption-desorption isotherm, pore size distribution, crystallinity, acidity and surface morphology. The composites CMA, CSA, CMS and CSS were characterized for their crystallinity, acidity and surface morphology.

HZSM-5 gave 98.5 wt% UPO conversion with 45.2 wt% yield of gasoline fraction and 25.9 wt% gaseous products. Composite CZA35 gave 97 wt% UPO conversion, 47 wt% yield of gasoline fraction and 19.7 wt% gaseous products as compared to HZSM-5. The alumina coating increased the average pore size (APS) of the mesopores and reduced the acidity of composite catalyst. Steam treated HZSM-5 and CZA35 showed comparable activity as the fresh catalysts. St-ZSM5 gave 93.5 wt%

UPO conversion with 46 wt% yield of gasoline fraction and UPO conversion was 92.3 wt% with 46.3 wt% yield of gasoline fraction over St-CZA35. The reduction in the surface area of St-CZA35 was lower as compared to St-ZSM5. The aromatics (BTX) present in the organic liquid product (OLP) were reduced from 33.9 wt% obtained with fresh CZA35 to 17.9 wt% over St-CZA35.

Composite CBS25 gave comparable gasoline fraction yield with 62.9 wt% CPO conversion as compared to 74.5 wt% CPO conversion over H-Beta. Its activity was improved after steam treatment with increase in CPO conversion to 74.7 wt% with gasoline fraction yield of 31.8 wt%. H-Beta activity dropped after steam treatment with drop in conversion from 74.5 wt% to 65.5 wt% and gasoline fraction yield from 26 wt% to 23.8 wt%. The coating of silica-alumina helped to increase the cracking activity and hydrothermal stability of the composite due to change in the surface morphology.

The coating of alumina improved Al-MCM-41 hydrothermal stability. St-CMA25 gave 62 wt% CPO conversion with 19.7 wt% gasoline fraction yield, higher than that obtained over St-AlMCM-41 (60.5 wt% conversion with 13.1 wt% gasoline fraction yield). The composites CSA, CMS and CSS gave low cracking activity due to changes in the surface morphology as observed from SEM analysis. Comparing the performances of all synthesized composites, CZA35 was found to be best cracking catalyst.

The deactivation of catalysts was studied by obtaining time on stream data with palm oil to catalyst ratio in the range of 8 to 16. Composites with alumina, CZA and CMA showed lower deactivation as compared to HZSM-5 and Al-MCM-41 catalysts. The deactivation data were fitted using suitable activity model and deactivation parameters were obtained.

CHAPTER 1

INTRODUCTION

1.1 PETROLEUM RESOURCES

Petroleum crude supply is limited and cannot be generated due to its finite resources. This fossil fuel has been in use for last two hundred years. It is estimated that the current known reserves of petroleum on earth will only be able to supply total world demand for the next 40 years (US Department of Energy, 2006). Since the world is running out of petroleum, therefore, it is important to start planning as to what kind of fuels one is going to use when these finite supplies are exhausted. Thus, research and development on alternative fuels is intensively carried out all over the world to meet the future needs.

1.2 ALTERNATIVE FUELS FOR FUTURE

There are large investments in developing alternative fuel source. The major alternative fuel sources for future are natural gas, hydrogen (fuel cell) and biofuel. In context of Malaysia, there are several technical and socio-economic uncertainties involved in the utilization of other than liquid fuel (Ma *et al.*, 1994). Long run feasibility is an important aspect of the nation's research and development efforts, but their immediate application on a commercial scale is limited.

Biofuel is liquid or gaseous fuel that can be produced from the utilization of biomass substrates and can serve as a (partial) substitute for fossil fuels (Giampietro *et al*., 1997). It is more attractive since it can be applied directly to the petrol or diesel engine which is currently in use. Besides that, with the increase in awareness and importance attached to environmental issues such as global warming, biofuel from plant oils such as canola oil, tall oil and jojoba oil which are free from nitrogen and

sulfur compounds (Katikaneni *et al.*, 1995) are the most promising raw materials for the production of alternative fuel.

Bio-diesel produced from vegetable oils has been well accepted and used in trucks and buses in western countries (US Department of Energy, 2006). Recently, the industrial plants for the commercial production of bio-diesel from palm oil have been licensed in Malaysia (MPOB, 2006a). There are more than 15 industrial units in the production of bio-diesel utilizing crude palm oil in Malaysia.

1.3 BIOFUEL FROM PALM OIL

Malaysia is one of the largest producer of palm oil in the world. Figure 1.1 shows the world major producers of palm oil year 2005 with total palm oil production of 33.3 million tonnes (MPOB, 2006b). Malaysia contributed about 45 % for total world output of palm oil. Malaysia is fortunate in having high yield and continuous supplies of palm oil which would easily support the creation of an eco-friendly, renewable and alternative fuel source. Given the huge potential for Malaysian agriculture to benefit from the revolution in ‘green’ fuel production, efforts are being put into place to generate bio-fuels to supplement fossil fuel use.

Since 1980s, Malaysia Palm Oil Berhad (MPOB) in collaboration with the local oil giant, PETRONAS, has begun to develop a patented technology to transform crude palm oil into a viable diesel substitute (Basiron, 2005). This process involves the transesterification of crude palm oil using methanol into palm oil methyl esters or palm bio-diesel. Finally, this palm bio-diesel has been commercialized in Malaysia by year 2006 (MPOB, 2006a). Over the years, MPOB has shown that palm oil methyl esters can be successfully used as biofuel either directly or as blends with petroleum-based fuels (Basiron, 2005) based on the experiments on diesel engines including Mercedez Benz engine for over 300 000 km. For implementation, a stage 1: supply and pumps

are made available to government and some private fuel depots, and a stage 2: implementation in the Klang Valley followed by major towns in the whole country has been done. In the future, stage 3 will showcase the model to Indonesia and to work for collaboration and discipline within the ASEAN context (Basiron, 2005).

There is also a growing interest to produce bio-gasoline from palm oil since majority of cars are running on the gasoline engine. This studies involving catalytic conversion of palm oil to liquid hydrocarbons using various shape selective zeolite catalysts (Twaiq *et al.*, 1999, 2002, 2003a&b, 2004; Ooi *et al.*, 2003, 2004a,b&c). In this process, cracking catalyst is the main key to directly convert palm oil to biofuel with high selectivity towards bio-gasoline. The choice and type of catalysts play very important role in the quality and yield of bio-gasoline produced from palm oil. There are constant efforts in this direction to develop different types of nanostructured catalysts to be used for this process.

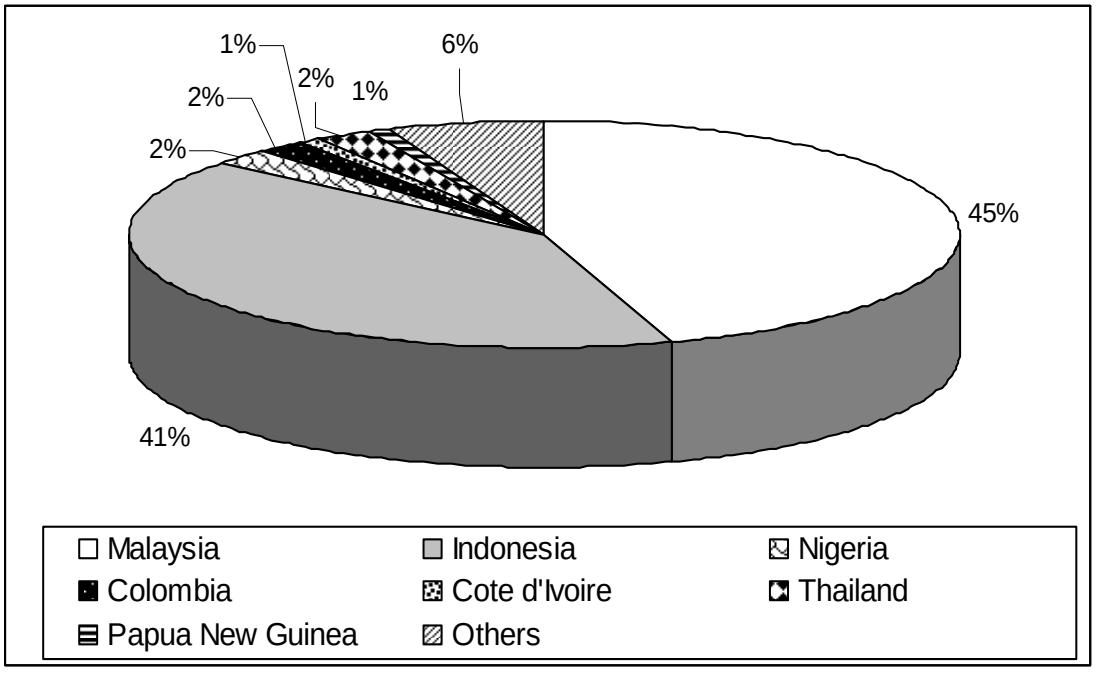

Figure 1.1: World major producers of palm oil 2005 (MPOB, 2006b).

1.4 NANOSTRUCTURED CRACKING CATALYSTS

The nanostructured materials are referred to porous materials with pore size is in nano range (< 100 nm). There are three types of porous materials classified according to their pore size range (Corma, 1997):

- Microporous material (< 2 nm)
- Mesoporous material (2 – 50 nm)
- Macroporous material (> 50 nm)

Different types of zeolites have been studied as cracking catalyst in order to find out the best catalyst in terms of the micropore structure that provide selectivity, and its tunable acidity, that can fit the requirement of the cracking process. Different zeolite based catalysts gave different activity and selectivity. The products distribution varied due to the shape selectivity effect and accessibility to the active sites. Besides the selectivity, hydrothermal stability of the catalyst is another criteria for a good cracking catalyst as industrial cracking process regenerates the used catalyst under steaming at high temperature. The reusability of the catalyst is also important factor to be considered in order to get an efficient and cost effective catalyst.

A large number of studies on the catalytic performance of microporous materials (zeolites) for cracking reactions have been explored for different kinds of hydrocarbon feedstocks, such as C_6-C_{10} olefins (Buchanan, 1998), n-heptane (Li *et al.*, 2000), cumene, n-propylbenzene and n-heptane (Nakao *et al*., 2004), vacuum gas oil (Corma *et al*., 1996) and heavy oils (Benazzi *et al.*, 2003) in order to obtain desired valuable hydrocarbons. ZSM-5 is the most studied microporous catalyst since it has high acidity compare to other microporous materials. It has been used as an additive in the commercial fluid catalytic cracking (FCC) operation in the petroleum refineries since its first application in catalytic cracking around 1983 based on its potential as booster of gasoline octane number (Buchanan *et al.*, 2001). The discovery of mesoporous

materials in 1992 (Beck *et al.*, 1992) has drawn a lot of attention in this area in order to overcome the limitation of microporous materials pore size to deal with bulky molecules. MCM-41 has tunable pore size in the range of 1.5-10 nm, high surface area (~1000 m^2/g) and high hydrocarbon sorption capacities (0.7 ml/g or greater) (Chen *et al.*, 2003) which is more suitable for processing of large hydrocarbon molecules. The next discovery of SBA-15 prepared under acidic conditions with pore size up to 30 nm was reported a few years later after MCM-41 discovery (Zhao *et al.*, 1998). This mesoporous material had better hydrothermal stability than MCM-41 due to its thicker wall. Although these mesoporous materials exhibited rather weak acidity strength similar to amorphous silica-alumina as compared to zeolites (Zhao *et al.*, 1996; Selvam *et al.*, 2001), introduction of trivalent atom into their mesostructure can increase the acidity and further enhance the cracking activity of the mesoporous materials. One of the limitations of this kind material is their lower hydrothermal stability as compared to zeolites (Zhao *et al.*, 1996; Selvam *et al.*, 2001).

A composite catalyst comprised of two different phases combining the advantageous of the individual catalyst components offers numbers of advantages in the cracking process. With the current interest on such materials provide bimodal pore systems that combine the benefits of each pore size, an opportunity for the development of more efficient cracking catalysts for the cracking of palm oil has to be explored. The composite catalysts containing both microporous (zeolite) and mesoporous materials as the cracking catalyst have been intensively studied due to their regular pore size of mesophase and strong acidity of the microporous zeolite. The mesoporous material in the composite catalyst has been found to improve the accessibility of the reactants to the active sites in zeolite (Twaiq, 2002; Ooi, 2004). At the same time, it is important to develop a composite catalyst with improved hydrothermal and thermal stability for the cracking of palm oil. The application of alumina and silica-alumina (low ordered meso or macroporous materials) in FCC

operation could lead the preparation of composite micro or mesoporous/macroporous in order to get better hydrothermal stability catalyst due to high stability of these two kind materials.

1.5 PROBLEM STATEMENT

A challenge faced in the development of the cracking catalyst is to meet the catalyst requirements such as hydrothermal stability at high reaction temperature, low coke formation and less gas production, good activity for bulky molecules, selective to desired product, and low cost due to increased catalyst usage rates. This development of an efficient catalyst may be met in part by adjusting the properties of the catalysts matrix (composite) without affecting their cracking activity.

The performance of mesoporous materials, MCM-41 and SBA-15 and their composite MCM-41 or SBA-15/microporous materials have been reported to give significant amount of gasoline yield in the catalytic cracking of palm oil (Twaiq, 2002; Twaiq *et al*., 2004; Ooi, 2004; Ooi *et al*., 2004c). However, the hydrothermal stability of these catalysts needs to be further improved and studied. Therefore, materials containing micro-macro and meso-macro pores need to be explored in order to have good hydrothermal stability and high reusability beside high selectivity towards gasoline. The well applied macroporous materials in FCC operation, alumina and silica-alumina could be selected for this purpose. The design of the right type of cracking catalyst is desired to achieve higher gasoline yield to make this process economically attractive for the commercial gasoline production in the future. The introduction of certain metal using suitable technique is also important in order to create acidity and suppress reactions responsible for the deactivation of catalysts due to coking.

1.6 OBJECTIVES

The present research study has the following objectives:

1. To synthesize nanostructured materials containing meso and macro pores and composite materials containing micro-meso, micro-macro and meso-macro pores.
2. To study the characteristics of synthesized nanostructured materials using different analytical techniques.
3. To study the catalytic activity of synthesized nanostructured composite materials as cracking catalysts for the conversion of used and crude palm oil and their selectivity for gasoline production.
4. To study the deactivation and regeneration of the catalysts in palm oil cracking reaction.

1.7 SCOPE OF THE STUDY

Two type of microporous materials, zeolite ZSM-5 (Si/Al = 40) and zeolite Beta (Si/Al = 12.5) and two types of mesoporous materials, MCM-41 and SBA-15 were studied and identified as the potential catalysts for the cracking of used palm oil and crude palm oil for the production of liquid fuel respectively. The selection is based on the past catalytic activity studies of these materials in palm oil cracking process (Twaiq, 2002; Ooi, 2004). The mesoporous materials MCM-41 and SBA-15 were successfully synthesized and characterized for their properties. Aluminum was introduced into these mesoporous materials to generate acidity.

The preparation of composite alumina/HZSM-5 or mesoporous materials in the granular form (diameter ~1-2 mm) was carried out using sol-gel method. The granulation was carried out by applying oil-drop method. The lower ordered mesophase alumina coated on HZSM-5 or mesoporous materials as outer layer of spherical composite (granule) and microporous or mesoporous materials as the core. Different weight ratio of the mesophase (alumina) and microphase (zeolite HZSM-5) or

mesophase (AlMCM-41/AlSBA-15) in the composite were prepared to see the effect of different percentages of different types of pore phases combined in the core-shell granule composite materials over its activity and hydrothermal stability in palm oil cracking. Composite silica-alumina/H-Beta or mesoporous materials were also synthesized using the seeding method with some modifications. These composites followed the core-shell concept of the catalyst on their particles.

Composite HZSM-5/alumina and H-Beta/silica-alumina were characterized for their BET surface area, pore size distribution, adsorption-desorption isotherm, crystallinity, acidity and morphology. While composite mesoporous materials with alumina and silica-alumina were characterized for their crystallinity, acidity and morphology.

The catalytic activity of the synthesized composite materials was carried out to identify their potential as catalyst in the cracking of crude and used palm oil respectively for the production of liquid fuel with interest in gasoline fraction. The used palm oil (UPO) was used as the feedstock for the cracking activity of HZSM-5 and its composite with alumina (CZA) in order to evaluate used palm oil as alternative source for a practical process without competing with the edible oil market. The crude palm oil (CPO) was used as the benchmark to the used palm oil to others catalysts. In order to evaluate their hydrothermal stability, the synthesized composite materials, zeolites and mesoporous materials were steamed at 1073 K for an hour and then evaluated their catalytic activity. The reusability of catalyst was evaluated using the regenerated sample. The spent catalyst was regenerated by burning the coke deposited on catalyst surface at 823 K prior to further catalytic cracking test.

The experiments were conducted at reaction temperature of 723 K, feed rate (WHSV) of 2.5 h^{-1} and crude/used palm oil to catalyst ratio of 8. The catalyst was

studied for the deactivation rate by obtaining time on stream data at feedstock to catalyst ratio in the range of 8 to 16. A suitable deactivation model was proposed and model parameters were determined.

1.8 ORGANIZATION OF THE THESIS

This thesis was divided into five chapters:

Chapter 1: Introduction is given about the world's fuel demand and the important of alternative fuels, the introduction of palm oil as the potential source for the production of biofuel through catalytic cracking and the role of cracking catalysts. The problem statement of the current research is stated to give the clear objectives of the present study. The scope of the study covers the research work done to meet these objectives.

Chapter 2: Literature review covers the characteristics, properties, synthesis, application and performance of microporous zeolites, mesoporous materials, and composite catalysts in catalytic cracking reaction. The deactivation studies of synthesized catalysts are also covered.

Chapter 3: Experimental methodology and analysis describes the particulars of the materials and chemical reagents used in the present work, the procedure for catalyst preparation and modification along with the characterization of the catalysts. The next part presents the palm oil catalytic cracking reaction consists of experimental setup, activity measurement of catalyst, deactivation study, hydrothermal stability study and products analysis.

Chapter 4: Results and discussion is divided into two parts: (a) Catalyst characterization and cracking activity of the synthesized catalysts and (b) Deactivation studies. The characteristic and the cracking activity of the synthesized catalysts are

presented and discussed comprehensively. The deactivation of catalysts based on the time on stream is presented. Deactivation model is developed by assuming catalyst activity (φ) is dependent on the time on stream (t) and the value of n_d and k_d was estimated using non-linear regression analysis method based on Levenberg-Marquard's algorithm. The experimental data are compared with the simulated data obtained from the deactivation model.

Chapter 5: Conclusions and recommendations cover the conclusions about the performance of synthesized catalysts as cracking catalysts for the production of gasoline from palm oil. The recommendations for the future studies are also given in this chapter.

CHAPTER 2

LITERATURE REVIEW

2.1 ZEOLITE, MOLECULAR SIEVES AND NANOSTRUCTURED MATERIALS

Zeolites are minerals comprised mostly of aluminum, silicon, and oxygen and having a crystal structure featuring spacious pores or rings (Bookrags, 2006). Zeolites were discovered and named in 1756 by Baron Cronstedt, a mineralogist (Vansant, 1990; Bookrags, 2006) but their molecular sieve properties were not observed until the mid 1920s. It was named from two Greek words for 'boiling stone' (zein-boiling, lithos-stone) which well describes the escape of water molecules from the cavities in natural zeolites (Bookrags, 2006).

Aluminosilicate zeolites comply with the following definition: "Crystallized solids characterized by a structure which comprises of:

- A three-dimensional and regular framework formed by linked TO_4 tetrahedra (T=Si, Al…), each oxygen being shared between two T elements,
- Channels and cavities with molecular sizes which can host the charge-compensating cations, water or other molecules and salts.
- The size of the synthetic crystals is generally between a fraction of a micrometer and several micrometers, but may reach several hundred micrometer. The diameter of the channels and cavities varies according to the structure from 0.3 to 1.3 nm, the highest values of the internal surface area and pore volume being 800 m^2/g and 0.35 cm^3/g respectively (Guth & Kessler, 1999).

McBan was the first who used the term ‘molecular sieves’ for the zeolite minerals, to explain the structural properties of these minerals by which the adsorbates could be admitted or rejected on the basis of molecular size (Vansant, 1990). International Union of Pure and Applied Chemistry (IUPAC) defined molecular sieve effect is the effect with respect to porous solids, where the surface associated with pores communicating with the outside space may be called the *internal surface*, because the accessibility of pores may depend on the size of the fluid molecules, the extent of the internal surface may depend on the size of the molecules comprising the fluid, and may be different for the various components of a fluid mixture (IUPAC, 2006). IUPAC has classified the molecular sieve materials based on their pore size into three categories (Corma, 1997):

- Microporous material pore size < 2.0 nm
- Mesoporous material 2.0 nm ≤ pore size ≤ 50.0 nm
- Macroporous material pore size > 50. 0 nm

From this pore size category, zeolites fall under group of microporous materials. In addition to zeolites (microporous material), there are many other materials possessing the characteristic of shape selectivity such as pillared clays which provide large-pore two-dimensional network, carbon molecular sieve with slit-shaped pores, metals and inorganic oxides which are very useful due to their pore structure (Sayari, 1996).

With the discovery of the natural zeolites, Barrer was the first to synthesize identical synthetic forms (Vansant, 1990). By 1953, more than 30 distinct pure zeolite species were synthesized. Since their development and introduction to industry in 1954 by the Union Carbide Corporation, these unique adsorbents have been used commercially in many systems for drying and purifying liquid and gaseous streams. In addition, zeolites have made possible the development of large-scale separation

processes used to recover normal paraffins from branched-chain and cyclic hydrocarbons. When properly modified, zeolites also have catalytic properties which in commercial applications are producing significant process improvements over conventional catalyst system (Vansant, 1990).

Nanostructured materials are referred as porous materials with structure having pores falling in the nano range, 10^{-9}. The general term “nanotechnology” deals with structures that are measured in nanometers. The nanotechnology has drawn attention to researchers from various fields since these nanomaterials provide potential applications which could not be achieved before with the life-size materials. Zeolites and also other types of molecular sieves could be categorized as nanostructured materials due to their pore diameter are in the nano range.

2.1.1 MICROPOROUS MATERIALS

Micropores in various materials may be random or ordered, and both are represented by large and important groups of commercially available products. They may be further subdivided into oxides and non-oxides; tetrahedrally oxygen coordinated, octahedrally oxygen coordinated and mixed oxygen coordination number structures; three dimensional (3D) and two dimensional (2D); single phase and multiphase, and so on (Vaughan, 1989). The linked 3D tetrahedral zeolite materials may be the most familiar, but the 3D linked tetrahedral-octahedral structures may be chemically and structurally more diverse, though less stable (Vaughan, 1989). Pore size ranges and maximum BET surface areas of several microporous materials are presented in Table 2.1.

Table 2.1: Important groups of inorganic microporous materials (Vaughan, 1989).

Material	Pore Size Range (nm)	Surface Area (m^2/g)
Zeolites	0.2-1.2	900
Layered intercallates	0.2-1.0	300
Pillared clays	0.5-2.0	400
3D octa-tetra framework	0.2-0.4	200
Gels	>2.0	800
Porous Carbons	>0.4	1000
Polyacid oxometalates	0.8-1.2	200

The search of new structure of microporous materials is still in progress although hundreds of different synthetic molecular sieves are available. Recently, new non-aluminosilicate, synthetic molecular sieves became available commercially. They include aluminophosphates (family of AlPO4 structures); silicoaluminophosphates (SAPO family); various metal-substituted aluminophosphates [MeAPO family, such as CoAPO-50 (AFY)]; and other microporous framework structures, such as crystalline silicotitanates (Sherman, 1999; Sayari, 1996). However, these ultra-large pore materials were found to be thermally unstable and having weak acidity as compared to aluminosilicates zeolite (Chen *et al.*, 1994; Csicsery, 1995).

2.1.1(a) Zeolite

Zeolite can be classified into four groups according to the pore diameter: small, medium, large and ultra-large pore zeolites (Sayari, 1996). The pore diameter of different zeolites depends on the number of tetrahedral in the ring around the pore with 8 tetrahedral as small-pore (0.4 nm), 10 tetrahedral as medium-pore (0.55 nm), 12 tetrahedral as large pore (0.8 nm) and more than 12 tetrahedral as ultra-large pore (1.8 nm).

The researchers at Mobil Oil Corporation worked with quarternary ammonium ions with longer alkyl chains, such as tetraethyl- or tetrapropylammonium, and thus obtained the first zeolites with Si/Al ratios more than 5. These were zeolites Beta and ZSM-5 with new structures. This race for high Si/Al ratios ended in 1978 with the synthesis of silicalite-1 which is the pure-silica end-member of ZSM-5 (Weitkamp *et al.*, 1999).

I. ZSM-5

ZSM-5 is Zeolite Socony Mobil which was discovered by Mobil Technology Corporation in 1965. It was first synthesized by Landolt and Argauer (Argaeur *et al*., 1972). This ultrastable synthetic siliceous crystalline material had an exceptionally high degree of thermal stability thereby rendering it particularly effective for use in processes conducted at high temperatures (Argaeur *et al*., 1972). The first scale commercial trial of ZSM-5 as cracking catalyst was done in a cracking unit in 1983 in the Neste Oy refinery, Naantali, Finland (Degnan *et al.,* 2000).

The framework of ZSM-5 contains a novel configuration of linked tetrahedral shown in Figure 2.1. It consists of eight five-membered rings. These ZSM-5 units join through edges to form chains. The chains can be connected to form sheets and the linking of the sheets lead to a 3D framework structure. The silicon can be substituted for aluminum without affecting the basic structure. The generic name “pentasil” has been given to designate these solids, irrespective of minor differences in crystal structure (Bhatia, 1990).

Silicon may be considered as the principal or key element of the framework. Elements which substitute for silicon must accept a tetrahedral coordination with oxygen. Aluminum is the element which replaces silicon most easily. The limits of the Si/Al ratio are 0.5 (e.g., bicchulite) and infinity (e.g., silicalite-1). The formation of the

framework charges is due to the replacement of the tetravalent silicon by trivalent or divalent elements. These charges contribute to the stabilization of the structure, through their interaction with the compensating cations which makes the synthesis easier. After synthesis, the cations present are normally alkali, alkaline-eatrh or R_4N^+ (R=H, alkyl, aryl) cations. The latter transform into protons during calcination, and can be exchanged (Guth & Kessler, 1999).

.

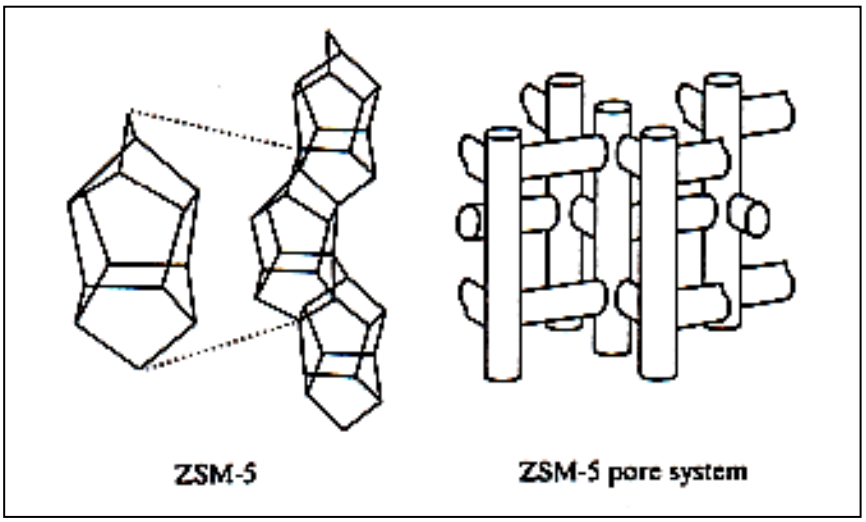

Figure 2.1: Framework structure of ZSM-5 (Gates, 1992).

II. Zeolite Beta

High silica zeolite beta with 3D twelve-membered ring channels was synthesized by Wadlinger early in 1967 for the first time (Wadlinger *et al*., 1967) while its structure was determine by Newsman and co-workers late in 1988 (Iza-Structure, 2006). The structure is formed with two-single pore rings and one 5-3 unit (Mostowicz *et al*., 1997). Zeolite Beta is characterized by a one dimensional channel system parallel to (001) with circular 12-rings apertures (7.6-6.4 Å) interconnected to a 2-dimensional channel system parallel to all crystallographically equivalent axes of the cubic structure (100) with the 12-rings apertures (4.5-5.5 Å). Zeolite Beta is disordered along the (100) axis. The disorder framework and the three simple ordered polytypes

are related to through layer displacement on (001) planes. Figure 2.2 shows the ring structure of zeolite Beta along different axis.

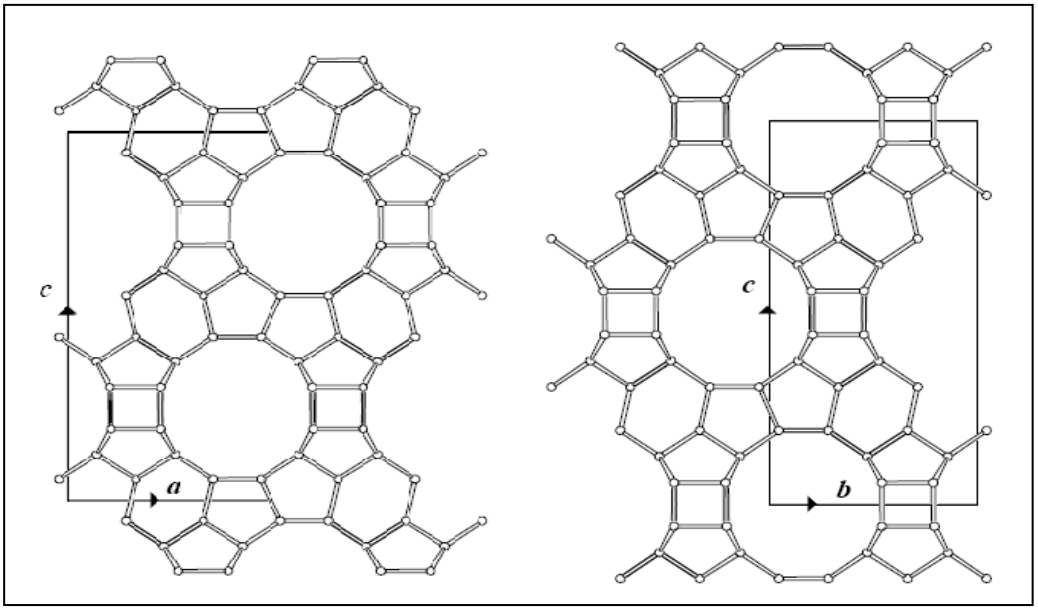

Figure 2.2: Pore structure in BEA along *b* (left) and *a* (right) axis (Iza-Structure, 2006).

Conventionally, the first synthesis used Na^+ and tetra-ethyl ammonium cation (TEA) as template in alkaline media with amorphous silica or silica sol as silica source (Mostowicz *et al*., 1997). The crystallization rate and crystal size of zeolite Beta depend on the alkalinity of gel and the molar fraction at each cation in Na^+ and K^- containing gels (Mostowicz *et al*., 1997; Zaiku *et al*., 2001).

2.1.1 (b) Zeolite as Cracking Catalyst

Modern cracking catalysts are made of some 20% zeolite dispersed in a matrix, which can be more or less active depending on formulation (Degnan *et al.,* 2000). In these catalysts most of the activity and selectivity comes from the zeolite, and therefore much attention was given to the study of optimization of this component. A large number of studies on the catalytic performance of zeolites for cracking reactions have explored the influence of pore structure, Si/Al ratios, types of acid sites present, coking characteristics, deactivation and regeneration of used catalyst were investigated.

I. ZSM-5

The applications of ZSM-5 as FCC additive into commercial operation gave dramatic change in FCC operation (Degnan *et al.*, 2000; den Hollander *et al.*, 2002; Buchanan *et al*., 2001). The quality of gasoline by increasing the gasoline octane number was obtained at the expense of the gasoline amount and was accompanied by an increased yield of light olefins. In palm oil cracking, Twaiq *et al.* (2004) found that the yield of gasoline fraction increased with the increase in Si/Al ratio of HZSM-5. This finding was consistent with Buchanan's (1998) work who observed higher gasoline selectivity in C_6-C_{10} olefins cracking using ZSM-5 FCC additive prepared with higher SiO_2/Al_2O_3 ratios. Different types and concentrations of metals loaded were studied in order to investigate different Bronsted acid sites strength and amount in the catalysts and their influence in the n-hexane cracking activity. It was found that H-Al-ZSM-5 gave highest cracking activity per Bronsted acid site compared to other catalysts (Liu *et al*., 2003a). Benazzi *et al.* (2003) studied the effect of the porous structure and the acidity of different acidic solids such as H-Y, H-β and H-ZSM-5 on the hydrocracking activity and selectivity of the transformation of heavy oils into valuable middle distillates via the hydrocracking of phenantrene on Pt-based catalysts. The results showed substantial differences in activity, which was correlated to acid site number. In the cracking of the gasoline-range olefins, ZSM-5 catalyst produced light olefins (LPG-range and some ethene) while the base FCC catalyst produced light olefins in lower amounts with small amounts of paraffins and the products were heavier than the gasoline feedstock. The differences between the two catalysts were the shape-selective mechanism where in the small pores of ZSM-5 only monomolecular cracking reactions took place, while in the larger pores of the FCC base catalyst, a bimolecular reaction mechanism occurred (den Hollander *et al*., 2002).

II. Zeolite Beta

Similar to ZSM-5, the shape selective properties of zeolite Beta also have octane-boosting capability in catalytic cracking and therefore have been used as an additive in FCC and also in upgrading gasoline (Mostowicz *et al*., 1997; Chen *et al.*, 2006). Zeolite Beta or known by its code as BEA (framework type code) has stronger acidity than conventional USY (ultrastable zeolite Y), however it seems to be difficult to make large mesopores like USY, but on the other hand it is easy to make BEA with small crystal size (Nakao *et al*., 2004). The synthesized zeolite Beta exhibited much higher activity than conventional and commercial zeolites in n-heptane cracking with the order of initial conversion of *n*-heptane cracking was as: BEA > ZSM-5> USY (Nakao *et al*., 2004). The differences of initial activities between zeolite Beta and other zeolites became much larger at lower reaction temperatures such as 773 K. In palm oil cracking, the limitation of microstructure of Beta for dealing with bulky molecules was improved by preparing composite MCM-41/Beta (Ooi *et al*., 2004c). This composite showed enhanced cracking activity with good selectivity of gasoline fraction.

2.1.2 MESOPOROUS MATERIALS

The discovery of M41S family (silica or aluminosilicate) by Beck *et al.* (1992) has created new opportunities in attempt to meet the increasing demand in both industrial and fundamental studies. Their extremely high surface areas and great accessibility of their pore systems really are the advantages. However, the amorphous nature of their pore walls made this type of mesoporous aluminosilicates little less thermal stable and these materials have much lower acidity than acid zeolites (Sayari, 1996). Further studies in mesoporous materials synthesis introduced HMS and MSU mesoporous materials by Pinnavaia group (Trong *et al*., 2001). They used two neutral routes based on hydrogen bonding and self assembly of non-ionic primary amines such as hexadecyl amine or polyethylene oxide (PEO) surfactants and neutral oligomeric silica precursors S^0I^0. The hexagon structure of this synthesized meso materials (HMS

and MSU) is not highly well ordered as compared to the mesostructured materials prepared by using ionic surfactant. However this material has a monodispersed pore diameter (ranging from 2.0 to 5.8 nm), thicker walls, a higher degree of condensation, and therefore a higher thermal stability. In addition, the mesopores of HMS being shorter allow a faster diffusion of reactants. While the third type of mesopores material, SBA-15 has been proposed by Stucky and co-workers (Zhao *et al.*, 1998; Trong *et al*., 2001) using a new approach involving amphiphilic di-and tri-block copolymers as organic structure directing agents and acid media amphiphilic di- or tri-block copolymer as the structure director agent. This material has larger pore (until 50 nm) and thicker wall (usually about 3-9 nm) which made it possesses good hydrothermal stability than other kind of mesostructured materials (Trong *et al*., 2001). The hexagonal structure of mesoporous materials is shown in Figure 2.3.

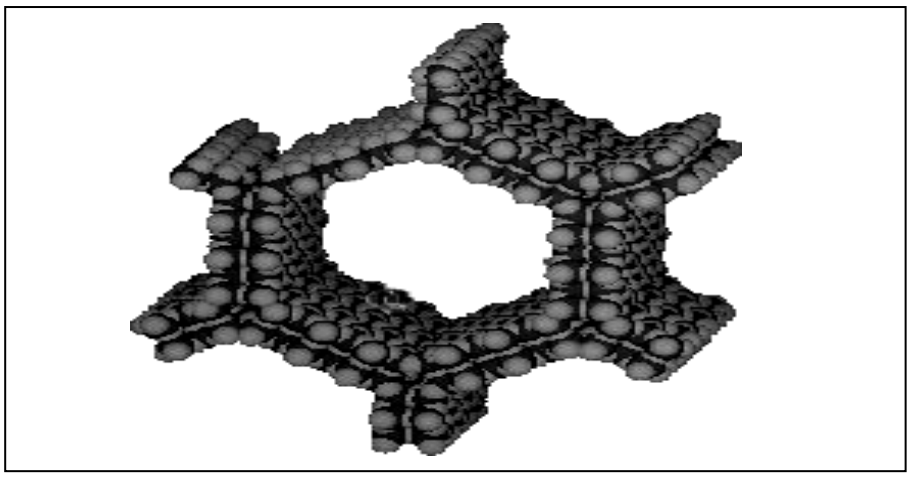

Figure 2.3: Hexagonal structure of mesoporous materials (Beck *et al*., 1992).

2.1.2(a) MCM-41

Since the discovery of MCM-41 by Mobil group (Beck *et al.*, 1992), various reviews (Sayari, 1996; Corma *et al*., 1996; Zhao *et al.*, 1996; Selvam *et al.*, 2001; Trong *et al.*, 2001) were reported regarding the synthesis, synthesis mechanism, properties and application of this material. This material with highly regular arrays of

uniform and tunable pore size (1.5–10 nm), extremely large surface area (> 700 m^2/g) and high thermal stability make it one of the most interesting materials in M41S family (Corma, 1997).

2.1.2(b) SBA-15

A family of highly ordered mesoporous (20-300 Å) silica structures have been synthesized by the use of commercially available nonionic alkyl poly(ethylene oxide) (PEO) oligomeric surfactants and poly(alkylene oxide) block copolymers in acid media (Zhao *et al*., 1998). SBA-15 mesoporous structures prepared has BET surface areas of higher than 700 m^2/g, pore sizes of 4.6-30 nm, silica wall thicknesses of 3.1-6.4 nm, and pore volumes as large as 2.5 cm^3/g which are hydrothermally stable as compared to MCM-41. In addition, the organic structure-directing agent, poly(alkylene oxide) triblock copolymer also to be good surfactant due to their amphiphilic character, low-cost commercial availability, nontoxic and biodegradability.

2.1.2 (c) Physicochemical Properties of Mesoporous Materials

I. Crystallinity

MCM-41 has amorphous walls despite of their long range periodic hexagonal structure (Sayari, 1996). X-ray diffraction (XRD) patterns of MCM-41 gave only a few distinct maxima in extremely low angles region (no larger than 2θ value of 6^o). The peaks included a very strong peak at the lowest angle (d_{100} reflection line) followed by three weaker peaks at higher angle (110, 200 and 210 reflection lines) that can be indexed on a hexagonal unit cell. The absence of the higher peaks and broadening of the remarkable peak in XRD pattern indicated the degradation of the ordered porous structure of MCM-41. Some MCM-41 exhibited only the 100 peak either because of too small scattering domain sizes or because of poorly ordered pore system (Sayari, 1996).

SBA-15 is also not a complete crystalline material and its X-ray diffraction (XRD) patterns are similar to that of MCM-41. Besides the d_{100} reflection line and three weaker peaks at higher angle (110, 200 and 210 reflection lines), SBA-15 also exhibited three additional weaker peaks in the range 2θ of 1^o to 3.5^o correspond to (300), (220) and (310) scattering reflection (Zhao *et al.*, 1998).

II. Acidity

Siliceous mesoporous materials have low acidity due to the silanol groups on the surface (Sayari, 1996). Acid sites, particularly Brønsted sites are the most desired active site for the hydrocarbon reactions. Their moderate acidity comparing to microporous materials could be overcome by substitution of silica by trivalent atoms such as Al^{3+} (Matsumoto *et al*., 1999; Trong *et al*., 2001; Jana *et al*., 2004; Ooi *et al*., 2004b; Kao *et al*., 2005; Zeng *et al*., 2005; Vinu *et al*., 2005), B^{3+}, Ga^{3+}, and Fe^{3+} (Trong *et al*., 2001). The active properties of aluminosilicate molecular sieves created from acidic sites which arise from the presence of accessible hydroxyl groups associated with tetrahedral aluminum in the silica matrix (Eswaramoorthi & Dalai, 2006). The incorporation of Al in mesoporous materials has been carried out by direct synthesis (Ooi *et al*., 2004b; Vinu *et al*., 2005) and post-synthesis (Oumi *et al*., 2001; Kao *et al*., 2005; Zeng *et al*., 2005) methods using different aluminum sources in order to create the desired acidity while keeping the mesoporous structure. The increase of aluminum content in mesophase resulted in a decrease of the well-defined hexagonal order, as observed from XRD bands and contraction of pore diameter upon calcination. To prevent the formation of structural defects, post-synthesis alumination has been found to be an effective method to prepare Al-containing MCM-41 with uniform pore structure.

However, it is very difficult to introduce the metal ions in the silica framework of SBA-15 directly due to the facile dissociation of metal–O–Si bonds under strong acidic hydrothermal conditions due to the too easy dissociation of Al–O–Si bond under acidic

hydrothermal condition and the remarkable difference between the hydrolysis rates of silicon and aluminium alkoxides (Eswaramoorthi & Dalai, 2006). Post-synthesis alumination carried by Zeng *et al.* (2005) using aluminum chloride aqueous solution was successively incorporated aluminum in the framework of SBA-15. Kao *et al*. (2005) claimed that post-synthesis alumination using $(NH_4)_3AlF_6$ solution as the aluminum source is easy and efficient. The resulted AlSBA-15 materials exhibited a high framework aluminum content (up to a bulk Si/Al ratio near 5), good structural and well-developed Bronsted acidity. The direct synthesis method also successively incorporated aluminum directly into the framework of SBA-15 (Ooi *et al.*, 2004b; Vinu *et al.*, 2005). However post-synthesis method can improve accessibility since acids are only located on the surface (not in the walls) and the uniformly hexagonal framework of mesoporous material was effectively maintained and found to be more effective over direct synthesis because of the strong acidic media involved during the synthesis of SBA-15 (Trong *et al.*, 2001; Oumi *et al*., 2001).

III. Hydrothermal Stability

It is believed that the steam stability of mesoporous is related to the thicker framework walls, the higher condensation of surface silanol groups and the presence of some arrangements of zeolite five-ring subunits in the framework walls (Fang *et al*., 2005). Therefore SBA-15 which has thicker wall having higher hydrothermal stability than MCM-41. MCM-41 has shown high thermal stability when water is absent but when expose to high temperature steam or boiling water, it loses its structure. The collapse of the structure has limited the applications of MCM-41 especially in the catalytic reactions involving aqueous solution. Although pure silica MCM-41 is more stable than aluminum containing MCM-41, but the lack of acid sites and ion exchange capability is one of the drawbacks for its practical industrial applications. There have been extensive efforts in improving the thermal and hydrothermal stability of MCM-41 besides improving the acidity. Several paths related to the improvement have been

reported. This includes pH adjustment (Ryoo & Kim, 1995; Lindlar *et al.*, 2000; Luechinger *et al.*, 2003), ion exchange (Kim *et al.*, 1995), post-treatment with phosphoric acid (Huang & Li, 2000), addition of sodium fluoride (NaF) (Kim *et al.*, 2000b) and preparation via neutral-cationic route using butylamine and cetyltrimethylammonium bromide as co-templating agents for MCM-41 (Fang *et al*., 2005). The synthesized mesostructure could retain its integrity after exposure to 20% (v/v) water vapor in Ar at 1073K for 4 h (Fang *et al*., 2005). All these methods were used to increase the hydrophobicity by increasing the aluminosilicate polymerization degree while decreasing the surface hydroxyl groups (Huang & Li, 2000). With pH adjustment and ion exchange, MCM-41 showed stability at 1170K in air and oxygen containing water vapor (Kim *et al.*, 1995). NaF addition in mesoporous materials synthesis, F^- ions were assumed to be a mineraliser replacing OH^- ions in the zeolite synthesis. The resulting MCM-41 was found to be stable even after it was boiled in water at 433K for 10 h (Kim *et al.*, 2000b). Hence, the replacement of hydroxyl group in order to create a chemically inert surface of MCM-41 is one of the effective methods to improve its hydrothermal stability. Higher temperature and longer aging time resulted in larger pore size with thinner pore wall and decreased the resistance of SBA-15 to steaming (Zhao *et al.*, 1998). The use of higher molecular weight amphiphilic block copolymers yielded SBA-15 with larger pore size and thicker pore wall, leading to enhanced hydrothermal stability. Sun *et al.* (2001) reported the synthesis of long-range order SBA-15 under basic conditions with higher stability. The sample had good thermal stability for 5 h at 1173 K and withstands more than 24 h in boiling water. Direct synthesis for the introduction of aluminum in SBA-15 yielded higher thermal and hydrothermal stability than pure siliceous SBA-15 and MCM-41 respectively (Yue *et al.*, 2000). After steaming at 723 K for 48 h, AlSBA-15 retained the same adsorption and desorption isotherms as well as the XRD patterns.